A Conductive Polymer Hydrogel Supports Cell Electrical Signaling and Improves Cardiac Function After Implantation into Myocardial Infarct

Anton Mihic, MSc; Zhi Cui, MSc; Jun Wu, MD; Goran Vlacic, BASc; Yasuo Miyagi, MD; Shu-Hong Li, MSc; Sun Lu, MD; Hsing-Wen Sung, PhD; Richard D. Weisel, MD; Ren-Ke Li, MD, PhD

Background—Efficient cardiac function requires synchronous ventricular contraction. After myocardial infarction, the nonconductive nature of scar tissue contributes to ventricular dysfunction by electrically uncoupling viable cardiomyocytes in the infarct region. Injection of a conductive biomaterial polymer that restores impulse propagation could synchronize contraction and restore ventricular function by electrically connecting isolated cardiomyocytes to intact tissue, allowing them to contribute to global heart function.

Methods and Results—We created a conductive polymer by grafting pyrrole to the clinically tested biomaterial chitosan to create a polypyrrole (PPy)-chitosan hydrogel. Cyclic voltammetry showed that PPy-chitosan had semiconductive properties lacking in chitosan alone. PPy-chitosan did not reduce cell attachment, metabolism, or proliferation in vitro. Neonatal rat cardiomyocytes plated on PPy-chitosan showed enhanced Ca^{2+} signal conduction in comparison with chitosan alone. PPy-chitosan plating also improved electric coupling between skeletal muscles placed 25 mm apart in comparison with chitosan alone, demonstrating that PPy-chitosan can electrically connect contracting cells at a distance. In rats, injection of PPy-chitosan 1 week after myocardial infarction decreased the QRS interval and increased the transverse activation velocity in comparison with saline or chitosan, suggesting improved electric conduction. Optical mapping showed increased activation in the border zone of PPy-chitosan–treated rats. Echocardiography and pressure–volume analysis showed improvement in load-dependent (ejection fraction, fractional shortening) and load-independent (preload recruitable stroke work) indices of heart function 8 weeks after injection.

Conclusions—We synthesized a biocompatible conductive biomaterial (PPy-chitosan) that enhances biological conduction in vitro and in vivo. Injection of PPy-chitosan better maintained heart function after myocardial infarction than a nonconductive polymer. **(*Circulation*. 2015;132:772-784. DOI: 10.1161/CIRCULATIONAHA.114.014937.)**

Key Words: conduction ■ injectable biomaterials ■ myocardial infarction ■ remodeling

Coronary heart disease is the leading cause of the rising incidence of heart failure worldwide.[1] Following myocardial infarction (MI), the limited regenerative potential of the heart causes scar formation in and around the infarction, leading to abnormal electric signal propagation and desynchronized cardiac activation and contraction.[2] The lack of electric connection between healthy myocardium and the scar with its islands of intact cardiomyocytes contributes to progressive functional decompensation. Injectable biomaterial has shown promise as an alternative biological treatment option after MI to reduce adverse remodeling and preserve cardiac function.[3,4] Among their many advantages, injectable materials can be delivered alone or as a vehicle carrying combination therapies, including cells or growth factors, and may provide mechanical and functional support to the injured heart. Over the past decade, several injectable biomaterials such as collagen,[5,6] alginate,[7] and fibrin[8] have been extensively studied.

Organic polymers that conduct electricity (conductive polymers) were first described in 1977, and this discovery was awarded the Nobel prize in 2000.[9,10] Conductive polymers are particularly appealing because they exhibit electric properties similar to metals and semiconductors while retaining flexibility, ease of processing, and modifiable conductivity. The electric properties of these materials can be fine-tuned by altering their synthetic processes, including the addition of specific chemical agents.[11] Biological applications of conductive polymers

Received December 15, 2014; accepted May 22, 2015.

From Division of Cardiovascular Surgery, Toronto General Research Institute, University Health Network, Ontario, Canada (A.M., Z.C., J.W., G.V., Y.M., S.-H.L. S.L., R.D.W., R.-K.L.); Department of Surgery, Division of Cardiac Surgery, University of Toronto, Ontario, Canada (A.M., Z.C., J.W., G.V., Y.M., S.-H.L. S.L., R.D.W., R.-K.L.); and Department of Chemical Engineering, National Tsing Hua University, Hsinchu, Taiwan (H.-W.S.).

Presented at the 2014 American Heart Association meeting in Chicago, IL, November 15 to 19, 2014.

The online-only Data Supplement is available with this article at http://circ.ahajournals.org/lookup/suppl/doi:10.1161/CIRCULATIONAHA.114.014937/-/DC1.

Correspondence to Ren-Ke Li, MD, PhD, MaRS Centre Toronto Medical Discovery Tower, 101 College St, Rm 3–702, Toronto, ONT, Canada M5G 1L7. E-mail renkeli@uhnresearch.ca

include transmitting electric impulses in neurite cultures,[12] regenerating nerves,[13] and healing wounds.[11] Cardiac applications to synchronize contractility in the injured myocardium have been suggested, but not functionally tested.[14] Injectable biomaterial can provide structural support to the injured heart, and a conductive injectable biomaterial may also be able to electrically bridge the scar barrier between healthy myocardium and viable cardiomyocytes within the scar. In this way, islands of cardiomyocytes within the infarct can be recruited and contribute to cardiac function. In addition, an injectable conductive biomaterial could provide direct electric activation of isolated contracting regions. Before now, no electrically conductive biomaterial has been used in cardiac applications to promote electric propagation across an infarction. Such a biomaterial would be hypothesized to synchronize ventricular contraction and substantially improve heart function post-MI.

Chitosan is biodegradable, produces minimal immune reaction in humans,[15] and has been used extensively as a biomaterial for the past 20 years. It has also proved useful as a scaffold to deliver cells[16] and as a carrier for drug delivery.[17] In the present study, we conjugated the conductive biomaterial polypyrrole (PPy) onto chitosan side chains to generate an electrically conductive PPy-chitosan hydrogel. We characterized this conductive biomaterial and showed that it is not toxic to cell growth or metabolism, can coordinate myocyte function ex vivo, and leads to significantly improved heart function when injected into rat hearts after MI.

Methods

Detailed methods can be found in the online-only Data Supplement.

PPy-Chitosan Biomaterial Preparation and Its Physical and Electric Properties

PPy-chitosan hydrogels were created in 2 concentrations (3:100 and 3:10 PPy:chitosan) by using an chemical oxidative polymerization method, and ungrafted chitosan (without PPy) was used as a control. Hydrogels were formed by using glutaraldehyde solution. Compression testing was used to determine the elastic modulus (n=4/group) and cyclic voltammetry was used to assess the electrochemical-dependent effects of voltage cycling on observed current amplitudes from each hydrogel (n=5/group). The electric conductivity (measured in S/cm) of chitosan alone and the 2 concentrations of PPy-chitosan was measured by using the 4-probe method. For all subsequent experiments, 3:10 PPy:chitosan was used, and is hereafter referred to as PPy-chitosan.

Biocompatibility of PPy-Chitosan

Rat smooth muscle cells (SMCs) were plated on uncoated polystyrene dishes or those coated with chitosan or PPy-chitosan at a concentration of 250 cells/mm^2 to assess cell attachment. After 48 hours, cells were fixed and stained with 4′,6-diamidino-2-phenylindole to visualize nuclei and to facilitate counting. SMC morphology was also examined by scanning electron microscopy.

To measure proliferation, rat SMCs were plated on polystyrene alone, chitosan, or PPy-chitosan at a density of 50 cells/mm^2. Cells were counted as above by using 4′,6-diamidino-2-phenylindole after 2, 5, or 10 days in culture. An 3-(4,5-dimethylthiazol-2-yl)-2,5-diphenyltetrazolium bromide assay was used to assess general SMC metabolism.

Ex Vivo Measurement of Bioconductivity Between Isolated Skeletal Muscle

All animal protocols were approved by the Animal Care Committee of the University Health Network. Rat leg skeletal muscle segments were isolated from the hind limbs of adult rats and plated 25 mm apart on dishes coated with chitosan or PPy-chitosan. An electromyogram recorder was used to obtain action potentials from 1 set of muscles, while stimulating electrodes were connected to the opposing muscle. Stimulation involved pacing the muscles at a constant voltage for 10 s at 1 Hz with 14-ms duration and gradually ramping the voltage amplitude every 10 s from 0.1 to 10 V, and the peak amplitude from the unstimulated muscle was measured in millivolts (n=6/group).

In addition to the 2 muscle-recording procedures, 1 muscle segment was excited with the use of noncontact stimulation by placing a positive electrode directly in the muscle, with the negative electrode placed into the hydrogel at a distance of 8 mm. Stimulation was gradually ramped from 0.1 V until a contractile response was elicited and could be visually detected in the muscle.

Isolation and Ca^{2+} Transient Assay of Neonatal Rat Cardiomyocytes

Neonatal rat cardiomyocytes were isolated from 1-day-old Sprague-Dawley rats and grown on control polystyrene plates, or those coated with chitosan or PPy-chitosan. Cardiomyocytes were loaded with the cell-permeable Ca^{2+} indicator Fluo-4 AM, fluorescent images of Ca^{2+} transient were recorded by using a high-speed electron-multiplied charge-coupled device camera, and isochronal maps were created.

Biomaterial Injection Into an Acute MI Model

Female Sprague-Dawley rats (225–250 g) underwent left descending coronary artery ligation and were allowed to recover. One week later, saline (n=6), chitosan (n=8), or PPy-chitosan (n=8) was injected into the peri-infarct region. ECGs were performed before infarction (–1), at the time of biomaterial injection (0), and 1, 2, 3, 4, 6, and 8 weeks after injection. Cardiac function was evaluated by using 2 techniques: echocardiography (ECHO) at several time points after MI, and pressure–volume (P–V) analysis at the 8-week end point. The following parameters were calculated by ECHO: left ventricular internal systolic dimension (LVIDS), left ventricular (LV) internal diastolic dimension, LV end-diastolic area, LV end-systolic area, percentage of fractional shortening, percentage of fractional area change, and percent ejection fraction. P–V analysis was used to determine percent ejection fraction, dP/dt, preload recruitable stroke work, end-systolic P–V relationship, and LV volumes.

Langendorff-Perfusion and Histological Examination of Isolated Rat Hearts

At the 8-week end point, the animals were euthanized and the hearts were retrieved for Langendorff perfusion (n=8 for chitosan- and PPy-chitosan–treated groups and n=6 for the saline control). Hearts were perfused on ice with the voltage-sensitive dye Pyridinium, 4-(2-(6-(dibutylamino)-2-naphthalenyl)ethenyl)-1-(3-sulfopropyl)-, hydroxide, inner salt 90134-00-2 (di-4-ANEPPS) dissolved in cardioplegia solution, electric conduction was measured by using an electron-multiplied charge-coupled device camera system, and isochronal maps were created. For videos, pseudocolored sequences were superimposed onto the raw video sequences to aid in the determination of cardiac anatomy with respect to electric activity.

Following optical mapping experiments, rat hearts were fixed in diastole, cross-sectioned, and stained with Masson trichrome. Whole-heart cross-sections were scanned with a 20× objective in the same transverse plane below the papillary muscles and scar thickness:LV area and scar area:LV area ratios were determined.

Statistical Analysis

Data are expressed as mean±standard error of the mean. For analyses where the variances were not found to be different, Student *t* tests were used for comparisons of means between 2 groups, and comparisons of means among ≥3 groups were performed with analysis of variance. If the analysis of variance *F* ratio was significant, differences were specified by Tukey or Bonferroni post hoc tests. For analyses where variances were not equal, differences between means were evaluated with an unpaired *t* test with the Welch correction for 2-group comparisons

or a Welch analysis of variance followed by Tamhane T2 post hoc testing for comparisons with ≥3 groups. For the ECG and echocardiography analysis, which consisted of repeated measures of the same animals over time, linear regression models adjusted for repeated measures through a compound symmetry covariance structure were performed using SAS v9.3 (SAS Institute, Cary NC). For the P–V analysis, the end-systolic P–V relationship and the preload recruitable stroke work were also compared between experimental groups by using linear regression models adjusted for repeated measures through a compound symmetry covariance structure with SAS v9.3. All other statistical analyses were performed with GraphPad Prism 5 (GraphPad, La Jolla, CA) or SPSS 23 (IBM, Armonk, NY) software. Differences were considered statistically significant at $P<0.05$.

Results

Characteristics of the PPy-Chitosan Hydrogel

To create an electrically conductive polymer, PPy was grafted onto chitosan at 2 different concentrations (3:100 and 3:10 PPy:chitosan) in the presence of $FeCl_3$ before polymerization by glutaraldehyde cross-linking to form PPy-chitosan hydrogels (Figure 1A and 1B). The PPy-chitosan, like chitosan alone, can be used to thinly coat tissue culture plates (Figure 1C). As shown in Figure 1D, the different concentrations of PPy-chitosan had similar tensile elasticity, suggesting they may have similar properties when used as a biomaterial in the context of the beating heart. When cyclic voltammetry was used to assess conductivity, both concentrations of PPy-chitosan formed hysteresis loops corresponding to their oxidative/reduction states, whereas ungrafted chitosan demonstrated a uniform linear relationship, suggesting that PPy-chitosan hydrogel has semiconductive properties, unlike chitosan alone (Figure 1E). Because the 3:10 PPy:chitosan concentration showed significantly higher conductivity than either 3:100 PPy:chitosan or ungrafted chitosan, 3:10 PPy:chitosan was used for all further experiments and is subsequently referred to as PPy-chitosan (Figure 1F).

Biocompatibility of PPy-Chitosan Hydrogel

Biocompatibility is a necessary characteristic of a cardiac biomaterial. Because cardiomyocytes have limited proliferation capacity in culture and are frequently overgrown by contaminating fibroblasts, we assessed the effects of PPy-chitosan on proliferation of SMCs, which are important for cardiac vasculogenesis after MI. To assess whether the addition of PPy to chitosan was toxic to cells, rat SMCs were grown for 2 days on plates coated with chitosan, PPy-chitosan, or directly on polystyrene plates as a control. The SMCs were then fixed, stained with 4′,6-diamidino-2-phenylindole and their confluence measured. No significant differences in cell density were associated with plating on polystyrene, chitosan, or PPy-chitosan, suggesting that PPy-chitosan did not inhibit SMC proliferation (Figure 2A and 2B). To demonstrate cell morphology and biomaterial attachment, SMCs grown on polystyrene, chitosan, and PPy-chitosan were examined by scanning electron microscopy. As shown in Figure 2C, the SMCs exhibited their typical spindle shape on both control and biomaterial-coated dishes. To further explore proliferation of SMCs grown on these different substrates, SMCs with the same initial seeding density were cultured on polystyrene plates and biomaterial-coated dishes for various times, and the numbers of SMCs/mm^2 were counted. No significant differences in cell density were seen between polystyrene plates and biomaterial-coated dishes (Figure 2D), indicating that SMCs can proliferate normally while cultured on PPy-chitosan. In an 3-(4,5-dimethylthiazol-2-yl)-2,5-diphenyltetrazolium bromide assay for overall cellular metabolism, SMCs grown on chitosan showed slightly reduced metabolism in comparison with SMCs grown on control polystyrene plates, whereas those grown on PPy-chitosan showed a significantly higher metabolic rate than controls (Figure 2E). Taken together, these results suggest that PPy-chitosan has no toxic effect on cell growth, proliferation, or metabolism in vitro.

Ex Vivo Electric Conduction Between Tissues With PPy-Chitosan Hydrogel

To ascertain whether PPy-chitosan could support conduction between tissues more effectively than ungrafted chitosan ex vivo, we developed an assay for bioconductivity between isolated rat muscles. Skeletal muscles (biceps femoris) isolated from adult rats were plated onto dishes coated with either PPy-chitosan or chitosan alone. To assay whether conduction could occur between them, the isolated tissues were placed at a distance of 25 mm apart, and one was stimulated using programmed electric stimulation, whereas the other was monitored by an electromyogram recorder to measure the action potential amplitude in the unstimulated tissue (Figure 3A and 3B). Plating the tissue samples on uncoated dishes produced no response in the unstimulated muscle, because the polystyrene dishes are electrically inert (data not shown). As shown in Figure 3C, plating on PPy-chitosan resulted in much higher action potential amplitude in the unstimulated muscle in comparison with plating on ungrafted chitosan at all voltages tested. We found that the threshold voltage required to elicit a contractile response in a single-muscle noncontact stimulation experiment was significantly lower in PPy-chitosan–embedded muscles (Figure 3D).

PPy-Chitosan Enhances Ca^{2+} Signal Conduction of Neonatal Rat Cardiomyocytes

To investigate whether chitosan alone or PPy-chitosan promotes electric conduction between spontaneous beating cardiomyocytes, we isolated neonatal rat cardiomyocytes and cultured them on both control dishes (uncoated) and dishes coated with biomaterial (chitosan or PPy-chitosan) for 5 days, and measured cytoplasmic Ca^{2+} transient propagation, an indirect indicator of action potential propagation. Cells were loaded with the Ca^{2+} indicator Fluo-4 AM to visualize increases in the intracellular concentration of calcium, which is correlated with myocyte contraction. As shown in Figure 3E and 3F, Ca^{2+} transient propagation was significantly faster in PPy-chitosan–plated cells than in control (uncoated dishes) and chitosan alone. This result suggests that PPy-chitosan significantly promotes the intrinsic Ca^{2+} propagation of cultured neonatal cardiomyocytes (n=4/group, $P<0.01$). Furthermore, this increase in calcium transient propagation is achieved without changing the shape or duration of the calcium transient (Figure 3G).

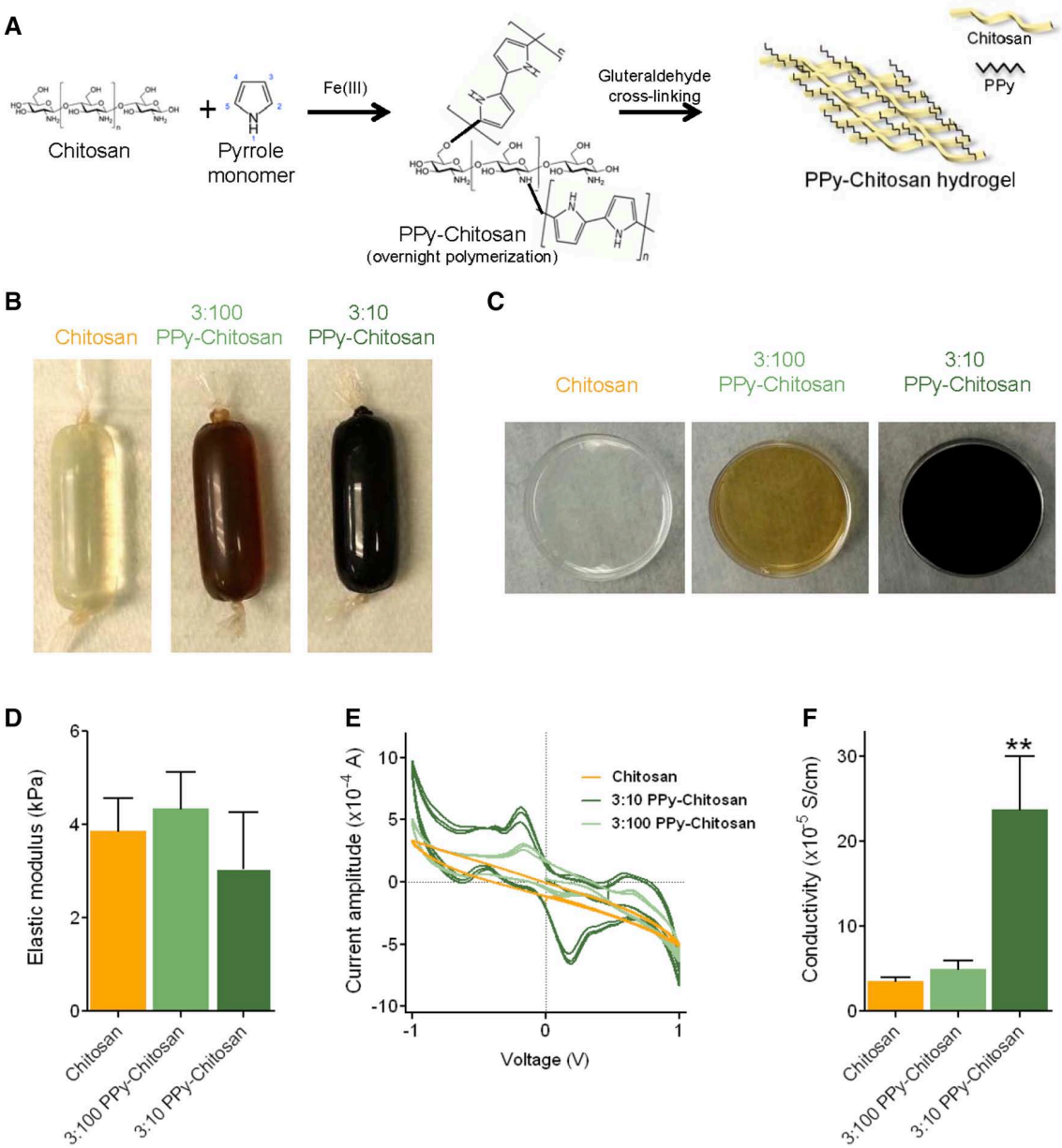

Figure 1. Polypyrrole (PPy)-chitosan hydrogel shows semiconductive properties in vitro. **A**, Schematic outlining the grafting of PPy monomers to chitosan and subsequent cross-linking to form a hydrogel. **B**, Dialysis bags containing chitosan and 2 concentrations of PPy-chitosan (3:100 and 3:10 PPy:chitosan). **C**, Hydrogels were thinly coated on the surface of 35-mm dishes. **D**, The elastic modulus was similar between chitosan and the 2 concentrations of PPy-chitosan. **E**, Cyclic voltammetry was used to assess the electrochemical and current-voltage properties of the hydrogels. Chitosan gel possesses a uniform linear relationship, whereas PPy-chitosan hydrogels form hysteresis loops corresponding to their oxidative/reduction states. **F**, Four-point probe measurements demonstrate that 3:10 PPy:chitosan was significantly more conductive than 3:100 PPy:chitosan or chitosan alone (n=6, $^{**}P<0.01$). 3:10 PPy:chitosan was used for all subsequent experiments.

Reduced QRS Interval and Improved Transverse Conduction Velocity in a Rat Model of MI

To determine whether injection of the conductive biomaterial PPy-chitosan is beneficial after cardiac injury, rats were injected with chitosan, PPy-chitosan, or a control saline solution 1 week after MI. ECGs were recorded before coronary artery ligation, at the time of biomaterial injection and 1, 2, 3, 4, 6, and 8 weeks later. At the time of the biomaterial injection, rats injected with PPy-chitosan or ungrafted chitosan showed normal ECG wave patterns, similar to saline-injected controls (Figure 4A). However, when the mean values were compared between experimental conditions, the saline or chitosan-alone groups had prolonged QRS intervals after infarction, whereas the PPy-chitosan–injected group had significantly reduced mean QRS intervals that were similar to pre-MI values (Figure 4B, $P<0.01$ for PPy-chitosan versus the other 2 groups). The QTc intervals were increased (owing to the current of injury) in all animals without any differences between groups. The narrower QRS interval may indicate more efficient conduction in post-MI hearts treated with PPy-chitosan in comparison with those treated with chitosan or saline.

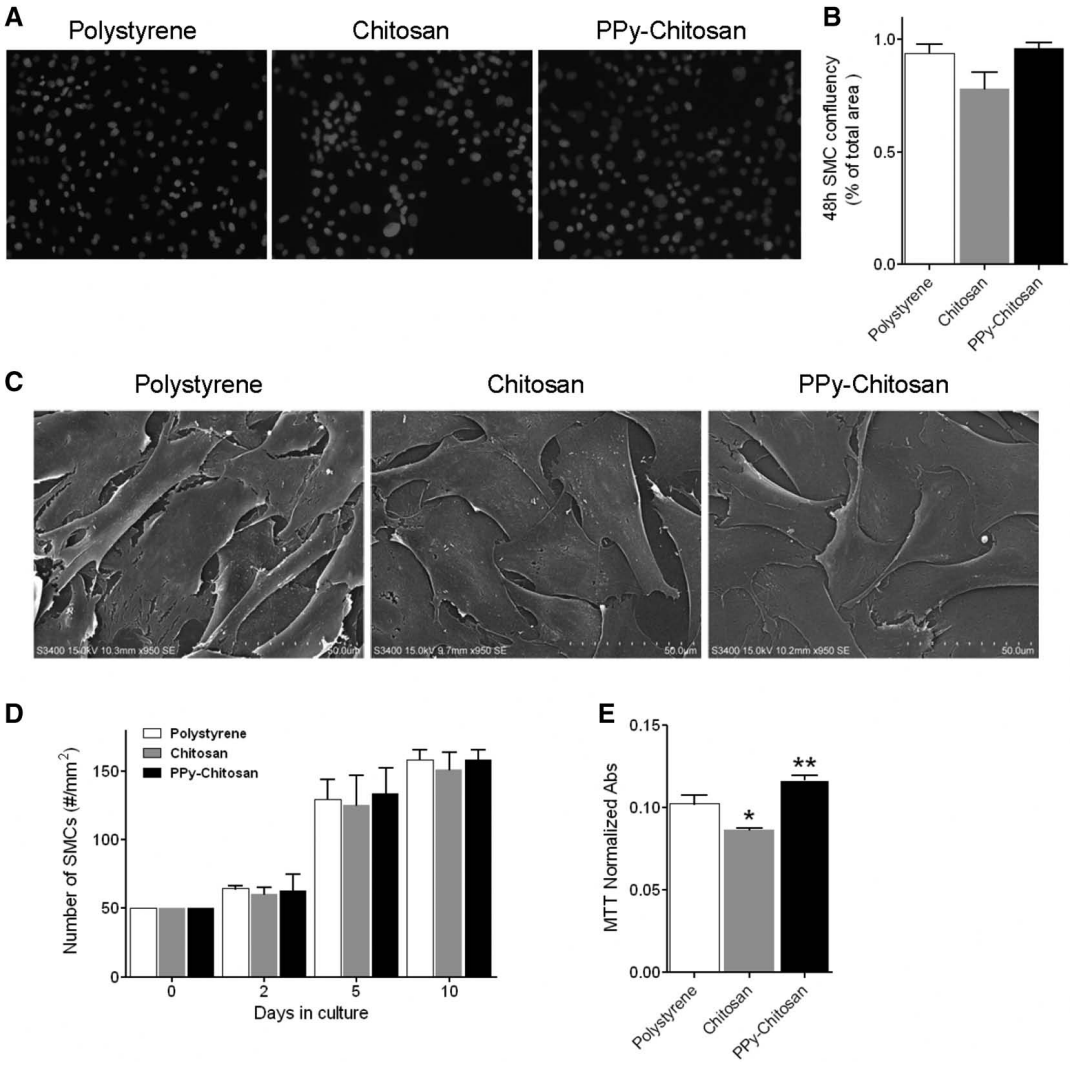

Figure 2. Polypyrrole (PPy)-chitosan hydrogel supports cell growth without toxicity. **A**, Rat smooth muscle cells (SMCs) were plated on polystyrene culture dishes alone or with a coating of chitosan or PPy-chitosan, grown for 48 hours, and then stained with 4′,6-diamidino-2-phenylindole (DAPI). **B**, Polystyrene, chitosan and PPy-chitosan all supported SMC cell growth to confluence at 48 hours with a similar cell area:total area ratio, suggesting there was no significant difference in the ability of the cells to attach to these substances. **C**, SMCs plated on polystyrene, chitosan, or PPy-chitosan showed normal cell morphology by scanning electron microscopy. **D**, Chitosan and PPy-chitosan supported SMC proliferation to a similar degree as polystyrene during 10 days in culture. **E**, An MTT assay demonstrated that PPy-chitosan supported enhanced SMC metabolic activity compared to cell growth on polystyrene alone (n=4, $^{**}P<0.01$) whereas growth on ungrafted chitosan slightly depressed SMC metabolic activity (n=4, $^{*}P<0.05$), suggesting PPy-chitosan did not produce any adverse cytotoxic-related effects. MTT indicates 3-(4,5-dimethylthiazol-2-yl)-2,5-diphenyltetrazolium bromide.

To directly assess cardiac conduction by optical mapping in biomaterial-injected animals, hearts from healthy rats (without MI), and those injected with saline, chitosan alone, or PPy-chitosan post-MI were excised at the end point of the study and Langendorff-perfused (Figure 4D through 4G, Movies I and II in the online-only Data Supplement). No significant difference in longitudinal conduction velocity was observed in the experimental groups, but rats injected with PPy-chitosan had significantly faster transverse conduction velocities than did saline- or chitosan-injected animals (Figure 4H and 4I). Indeed, the transverse conduction velocity in the PPy-chitosan–injected rats was similar to those without MI. Significantly greater conduction velocity in the border zone/scar region was also seen in PPy-chitosan–treated hearts in comparison with saline alone (Figure 4J). We also found that PPy-chitosan–treated hearts had differently shaped scars than those injected with saline or chitosan. They were more tapered in the longitudinal direction of conduction in comparison with the more rounded shape seen in saline- or chitosan-injected hearts (Figure 4E through 4G). These results suggest that PPy-chitosan injection improves the efficiency of cardiac conduction after injury.

Measurement of LV Function

Cardiac function was evaluated by using 2 techniques: echocardiography (ECHO) at several time points after MI, and P–V analysis at the end of the study (8 weeks postinjection). Left coronary ligation resulted in significant LV dilatation and progressive ventricular dysfunction, as assessed by ECHO (Figure 5A). All ECHO parameters were indistinguishable among the experimental groups at the time of biomaterial injection (week 0, Figure 5B through 5D) because of the

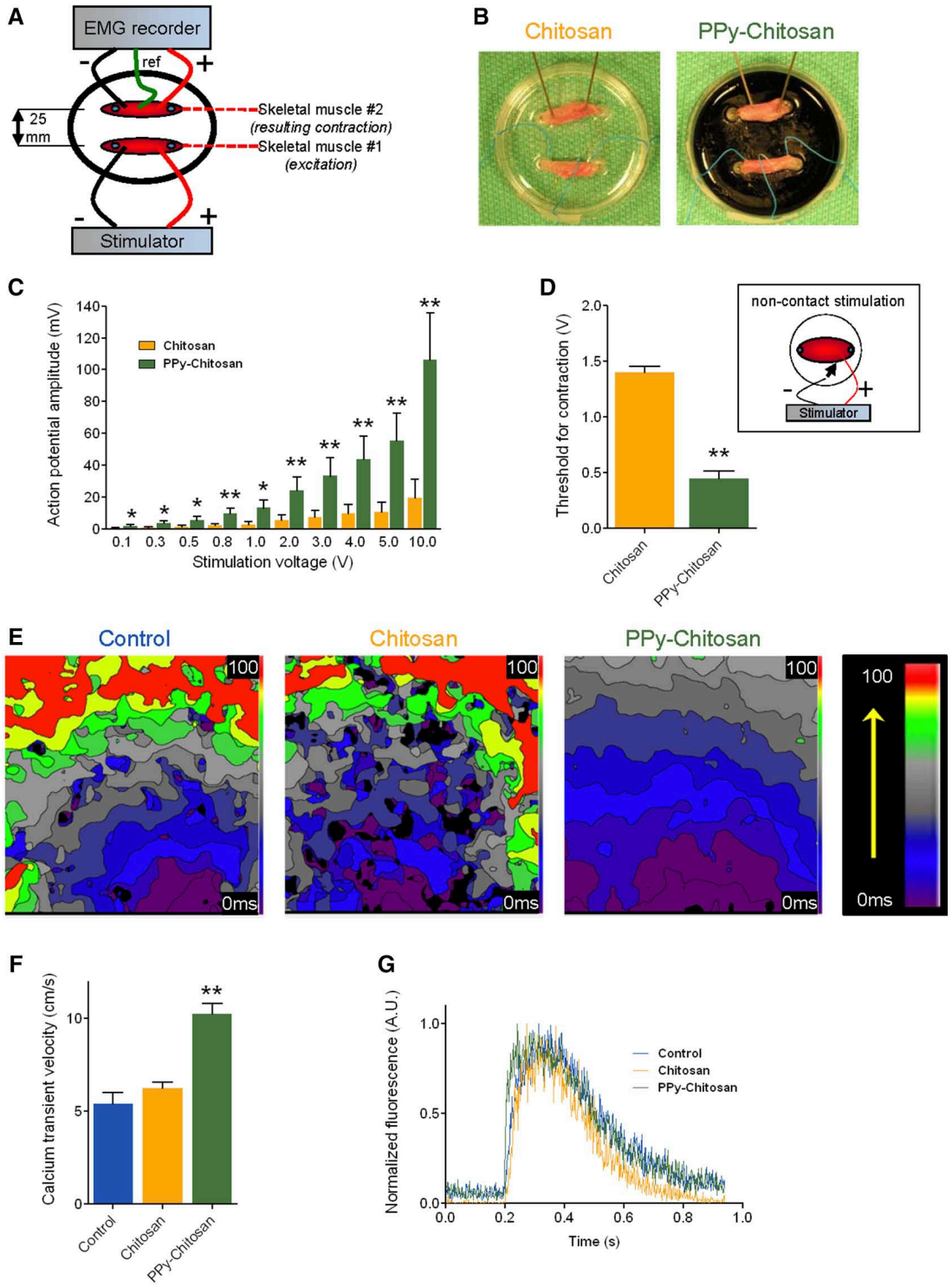

Figure 3. Polypyrrole (PPy)-chitosan hydrogel enhances skeletal muscle stimulation at a distance and enhances calcium transit velocity in neonatal cardiomyocytes. **A**, Schematic of the ex vivo skeletal muscle excitation assay. Rat leg skeletal muscle strips (biceps femoris) were plated on chitosan or PPy-chitosan 25 mm apart. One muscle was electrically stimulated while the other was attached to an electromyography (EMG) recorder to detect elicited action potentials. **B**, Photograph of the assay outlined in **A**, with chitosan- (**left**) and PPy-chitosan–coated plates (**right**). **C**, The skeletal muscle strips on PPy-chitosan had significantly greater action potential amplitudes recorded from the recipient unstimulated muscle than the strips on chitosan alone over the range of voltages evaluated (n=6/group, $^{*}P<0.05$, $^{**}P<0.01$). **D**, Noncontact stimulation of a single skeletal muscle was used to determine the threshold voltage for contraction (see schematic, Inset). The PPy-chitosan threshold voltage was significantly lower than that for chitosan (n=6/group, $^{**}P<0.01$). **E**, Optical mapping of calcium wave propagation through rat neonatal cardiomyocytes grown to confluence on polystyrene (control), chitosan, or PPy-chitosan plates. Calcium propagation was faster and more consistent over the area of the plate with fewer islands of stalled or delayed propagation in cardiomyocytes plated on PPy-chitosan in comparison with plates covered with ungrafted chitosan or control plates. **F**, Rat neonatal cardiomyocytes plated on PPy-chitosan showed significantly faster calcium transit velocities than those grown on control (polystyrene) or ungrafted chitosan (n=4/group, $^{**}P<0.01$). **G**, Representative calcium transients demonstrate that there are no significant differences in the overall shape or duration of calcium waves among the 3 groups, despite the faster propagation observed in on PPy-chitosan.

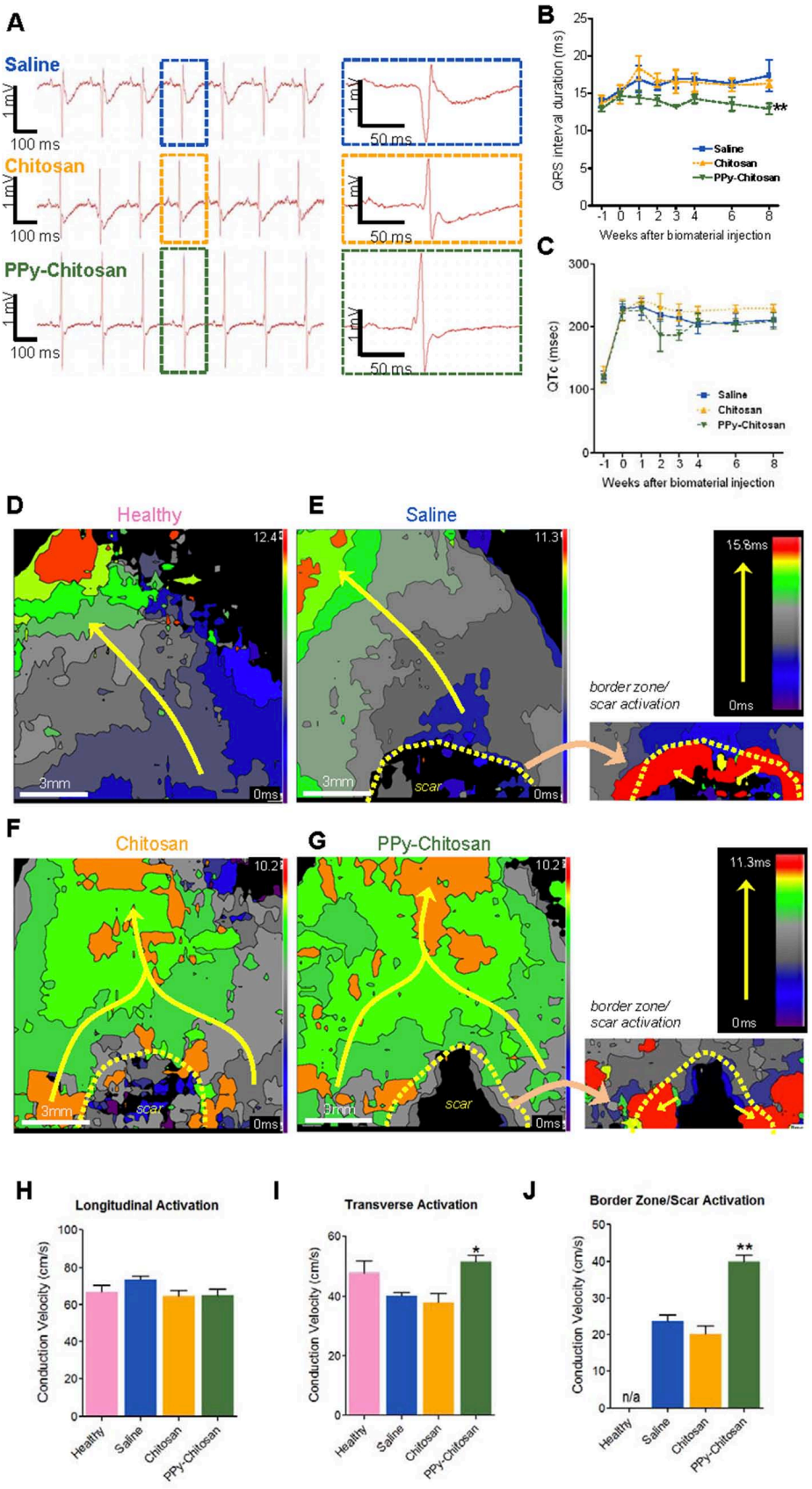

Figure 4. Polypyrrole (PPy)-chitosan hydrogel injection into the border zone postmyocardial infarction (MI) reduced QRS intervals and augmented transverse and border zone conduction velocities in comparison with chitosan alone. Saline, chitosan, or PPy-chitosan was injected into the border zone of rats 1 week post-MI (saline, n=6; chitosan, n=8; PPy-chitosan, n=8). **A**, Representative surface ECGs taken 8 weeks postinjection had normal waveform shapes in all groups. **B**, PPy-chitosan injection significantly maintained the normal QRS interval in comparison with the prolonged QRS intervals seen in the saline or chitosan-injected controls (**P<0.01 vs the other 2 (*Continued*)

preselection of animals within the selected percent fractional shortening range of moderate ventricular dysfunction. Mean fractional shortening and LVIDS were significantly improved in both the chitosan and PPy-chitosan groups compared to saline-injected animals (Figure 5B and 5C, $P<0.01$ for saline alone versus the other 2 groups for both parameters). Although there was no significant difference in either average fractional shortening or average LVIDS between the chitosan- and PPy-chitosan–injected groups, there was a significant difference in the slope of the change in fractional shortening and LVIDS over time between the PPy-chitosan group and both chitosan and saline alone, indicating that PPy-chitosan injection better maintained heart function over time in comparison with the other 2 groups ($P<0.01$). Mean LV internal diastolic dimension was significantly improved in both the chitosan- and PPy-chitosan–injected animals in comparison with saline alone ($P<0.01$ for saline injection versus the other 2 groups) but there was no significant difference between chitosan or PPy-chitosan for this parameter (Figure 5D). There were also no significant differences in the slope of the change in LV internal diastolic dimension over time among the experimental groups.

Ventricular volumes and cardiac function were also evaluated by P–V analysis with load-dependent and load-independent parameters (Figure 5E through 5J). Eight weeks after injection, rats receiving chitosan showed significant improvement in several load-dependent measures, including percent ejection fraction, dPdt Max, and dPdt Min in comparison with saline controls, and PPy-chitosan demonstrated still further improvement (Figure 5E through 5G). In comparison with saline, chitosan improved the end-systolic pressure volume relationship (Figure 5I) and preload recruitable stroke work (both load-independent indices, Figure 5J), and PPy-chitosan further improved these parameters, indicating greater global contraction. Taken together, these functional results suggest the use of a conductive biomaterial post-MI better maintained heart function than the use of a nonconductive biomaterial.

Biomaterial Reduces Infarct Scar Size Post-MI

In Figure 6A, an intraoperative photograph shows PPy-chitosan injected into the border zone region of the heart. The 3 darker areas are the 3 sites of peri-infarct biomaterial injection. Eight weeks after biomaterial treatment, hearts were excised at physiological pressures, and the scar thickness and total scar area were analyzed. Injection of both chitosan and PPy-chitosan reduced scar size in comparison with saline control, but there was no significant difference in either scar area or thickness between the 2 biomaterials (Figure 6B through 6D). In PPy-chitosan–treated hearts, PPy-chitosan was still visible in Masson trichrome–stained heart sections after injection (Figure 6E), suggesting that the biomaterial was retained for at least 8 weeks after its injection and may continue to influence heart conduction throughout this time.

In summary, we engineered a conductive biomaterial by grafting pyrrole moieties onto chitosan before hydrogel cross-linking. We optimized the concentrations of this PPy-chitosan biomaterial, which demonstrated greater conductive potential in vitro than chitosan alone and supported the attachment of cells in vitro without toxicity or diminished proliferation. Plating on PPy-chitosan improved conduction between ex vivo skeletal muscle strips at a distance and promoted faster propagation of rat neonatal cardiomyocyte calcium transients. When injected into rat hearts after MI, PPy-chitosan reduced QRS interval, increased transverse conduction velocity, and improved heart function in comparison with ungrafted chitosan, suggesting that PPy-chitosan has the ability to improve conduction in the heart after injury.

Discussion

Ventricular dysfunction after an MI frequently progresses to heart failure, which is a major cause of morbidity and mortality despite advances in clinical management.[18,19] After MI, cardiomyocyte death results in a noncontractile fibrotic scar and altered electric properties, including delayed impulse propagation across the scar region, which contributes to ventricular dysfunction. Because adult cardiomyocytes have a limited regenerative capability after an MI,[20] new treatment strategies are required to preserve ventricular function and prevent adverse remodeling. We and others have previously reported that matrix biopolymers (eg, fibrin glue, collagen, and hydrogels) have shown much promise in preserving cardiac function after an MI, providing structural support to prevent thinning and dilation of the infarct scar.[21–23] In a rat model, injectable hydrogels such as thermally responsive chitosan have been shown to improve cardiac function and prevent dilation after MI.[24]

Chitosan has been used extensively as a biomaterial over the past 20 years and has been shown to be an excellent wound-dressing material because of its porous structure.[15,25] It has also been shown to have intrinsic antibacterial properties,

Figure 4 Continued. groups for comparison of means). No significant difference was seen in the change in QRS interval over time among the experimental groups. **C**, The QTc interval was prolonged and not different between groups after MI. Eight weeks after injection, hearts were excised and perfused on a Langendorff apparatus. Optical mapping was performed to visualize conduction, and representative images are shown for healthy animals (no MI; **D**), and animals injected with saline (**E**), chitosan alone (**F**), and PPy-chitosan (**G**) 8 weeks post-MI. The scar is outlined in yellow dashes, and arrows depict the direction of electric impulse propagation. PPy-chitosan hearts showed faster, less interrupted impulse conduction in areas adjacent to the scar than did chitosan or saline controls. The shape of the scar was also distinct in PPy-chitosan–injected hearts, with a more tapered morphology in the direction of longitudinal conduction in comparison with the more rounded scars seen in controls. Representative isochronal maps show details of conduction in the border zone surrounding the scar a few milliseconds after the initial activation for PPy-chitosan and the saline control. In this example, impulse conduction to the viable myocardium around the scar took <15.8 ms in the saline control and <11.3 ms in the PPy-chitosan–injected animal. Quantification of the optical mapping results showed no significant differences in longitudinal conduction velocity between experimental groups (**H**), but transverse conduction velocity was delayed in the saline and chitosan groups and significantly faster in the PPy-chitosan group and was at least as fast as in the normal heart (**I**), indicating more efficient conduction around the scar in PPy-chitosan–injected hearts (n=5 for the saline-injected group and n=6/group for chitosan and PPy-chitosan groups, $^{*}P<0.05$). **J**, Conduction velocity in the border zone leading to activation of the scar region was significantly faster in PPy-chitosan–injected hearts than in hearts injected with saline or ungrafted chitosan ($^{**}P<0.01$).

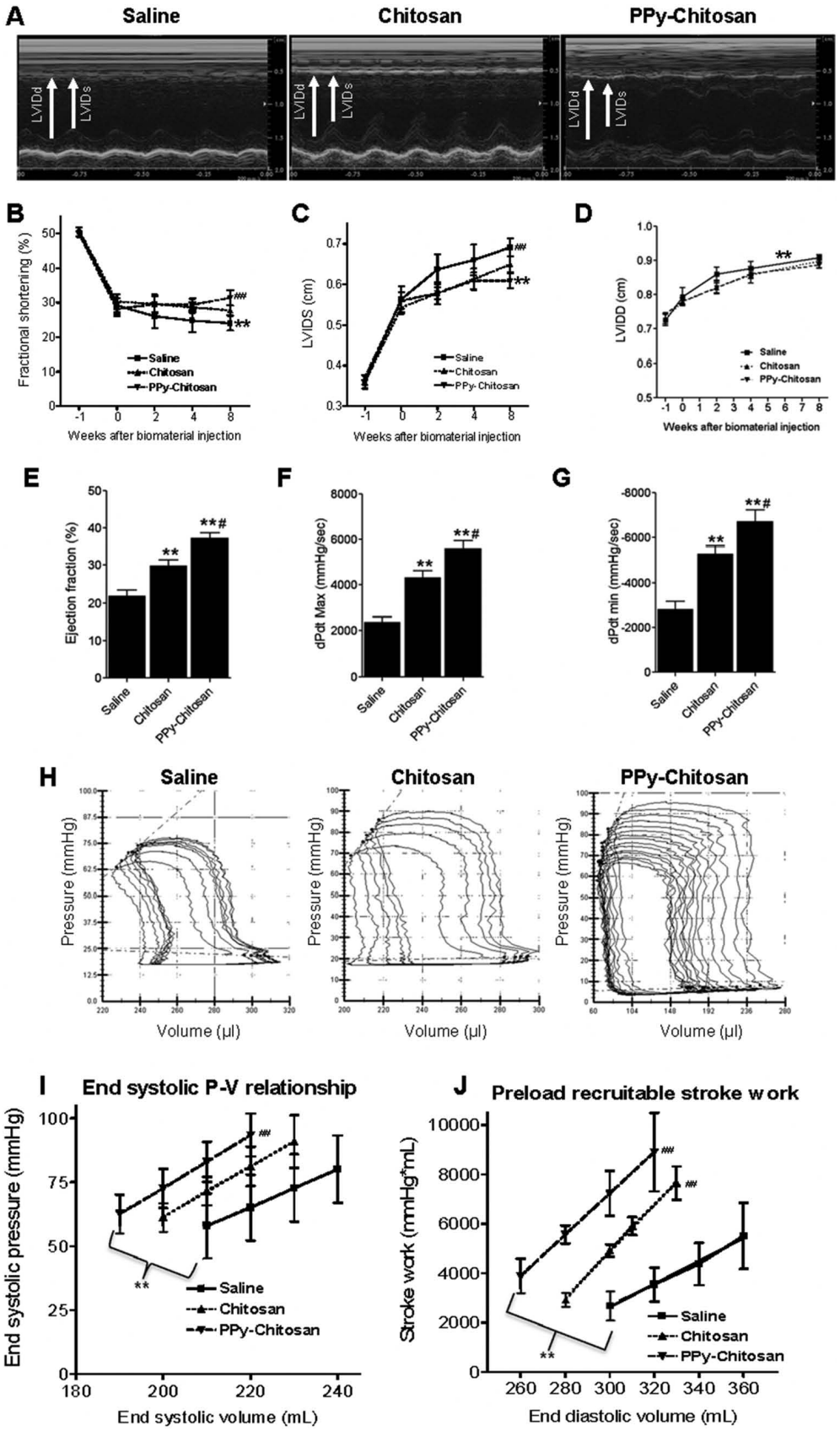

Figure 5. Systolic ventricular function was improved after polypyrrole (PPy)-chitosan hydrogel injection into the border zone. Saline, chitosan or PPy-chitosan was injected into the border zone of rats 1 week post-MI (saline, n=6; chitosan, n=8; PPy-chitosan, n=8). Echocardiography (ECHO) was performed at the time of MI (–1), at the time of injection (0), and 2, 4, and 8 weeks postinjection. **A**, Representative ECHO images 8 weeks after saline or biomaterial injection demonstrated that the PPy-chitosan group had the smallest left ventricular internal systolic dimension (LVIDS). When comparing mean fractional shortening (**B**) and LVIDS (**C**) among experimental (*Continued*)

is biodegradable, and produces minimal immune reaction in humans.[15] Chitosan has proved useful as a scaffold to deliver cells[16] and as a carrier for drug delivery.[17] Moreover, previous studies have shown that the injection of a chitosan hydrogel mixed with nuclear-transferred embryonic stem cells into the LV wall of a rat model following MI improved transplanted cell retention, and cardiac function, as well.[26]

Although injectable biomaterials benefit cardiac function by preventing ventricular dilation and enhancing myocardial regeneration, the contraction and relaxation of the heart depends on the conduction of electric impulses through cardiac tissue, and conduction velocity is reduced and repolarization is delayed in the infarct region following an MI.[27] Abnormal electric conduction in the infarct myocardium has not been investigated, and no previous study has evaluated an electrically conductive biomaterial for cardiac application to promote electric propagation across an infarction site. Such a biomaterial would be hypothesized to synchronize ventricular contraction and substantially improve heart function post-MI. We believe that an injectable conductive polymer may restore synchronous contraction following an MI by modifying the impulse propagation through the infarcted zone and permitting appropriately timed contraction of viable myocardium isolated by the infarct scar.

In this study, we chemically modified chitosan with the charge-carrying conductive polymer PPy yielding a biomaterial (PPy-chitosan) with >100× the conductivity of chitosan alone. We tested this new PPy-chitosan both in vitro and in vivo. In our rat model of MI, prolonged QRS duration was prevented, cardiac function was enhanced, and systolic volume was smaller in PPy-chitosan–treated hearts than in controls. In addition, optical mapping demonstrated that PPy-chitosan–treated hearts had faster transverse conduction velocities measured along the border zone epicardial surface. These findings suggest that this new conductive polymer improved coordinated heart beating and may represent an important tissue-engineering advance that could improve myocardial recovery.

The use of injectable hydrogels to support damaged ventricles and prevent heart failure is being explored in the clinic.[28] Conductive hydrogels such as PPy-chitosan may represent an improvement over the nonconductive hydrogels currently being explored, particularly for patients with a wide QRS complex and evidence of delayed regional contraction after an MI. It is also possible that PPy-chitosan may have other future uses in the clinic as an adjuvant therapy to biological pacemakers. Preclinical work has explored the transplantation of genetically modified cells to correct the types of arrhythmias currently treated using electronic pacemakers,[29,30] and coinjection with PPy-chitosan may enhance the function of the transplanted cells in their new environment.

Conductive polymers are a special class of organic materials that are capable of transmitting electric currents. Our PPy-chitosan conductive polymer is biocompatible and permits cell adhesion, and is therefore suitable for tissue-engineering applications. Our data demonstrated that PPy-chitosan injection after MI improved cardiac function in comparison with saline control or chitosan alone. The mechanism by which PPy-chitosan improves function has not been established in this study, but the electric conductive property of the PPy may have contributed to the beneficial effects. PPy is a polycationic, electrically conductive polymer. This particular feature of the polymer may contribute to restoration of the lost electric conductivity in the scarred peri-infarct region. Previous studies have shown that neurons grown on a PPy film show enhanced proliferation and differentiation in the presence of an electric stimulus.[12,31] Previous in vivo studies showed that PPy was not cytotoxic[32] and may regenerate damaged nerve tissue.[12] We have recently reported that isolated cardiomyocytes could grow on aligned composite conductive nanofibers of polyaniline and show synchronized beating.[33] In this study, optical mapping showed that chitosan-PPy–treated hearts had faster transverse conduction velocities along the border zone epicardial surface. This enhanced conduction velocity and repolarization in the peri-infarct regions could facilitate synchronous contraction thereby improving cardiac function.

This preliminary, proof-of-concept study has some limitations. Our in vitro experiments were done on stiff, thin layers of biomaterial owing to the technical limitations associated with visualizing experiments done on thicker layers of dark-colored PPy-chitosan, and because the beating of the neonatal cardiomyocytes tended to disrupt the surface of less-stiff, thicker gels. Neonatal cardiomyocytes function best on surfaces that closely mimic the elastic modulus of their native extracellular matrix,[34] and the thin coatings used in our in vitro neonatal cardiomyocyte assays are likely stiffer than is optimal for this cell type.[35] Future work could aim to generate PPy-chitosan gels with optimized elastic properties.

Figure 5 Continued. groups, chitosan, and PPy-chitosan injection showed significant improvement in comparison with saline alone, whereas no significant difference was seen between chitosan- and PPy-chitosan–injected animals (***P*<0.01 vs the other 2 groups). However, there was a significant difference in the slope of the change of both fractional shortening and LVIDS over time in PPy-chitosan–injected animals in comparison with chitosan or saline alone (##*P*<0.01 vs the other 2 groups). **D**, The mean left ventricular internal diastolic dimension (LVIDD) was significantly decreased in both chitosan and PPy-chitosan groups (***P*<0.01 for saline vs the other 2 groups) but there were no significant differences in the means between the chitosan and PPy-chitosan groups or in the slope of the change in LVIDD over time among any of the experimental groups. Volumetric data taken using pressure–volume (P–V) loops at 8 weeks postinjection showed that % ejection fraction (**E**), dPdt Max (**F**), and dPdt Min (**G**) improved significantly after injection with chitosan in comparison with saline controls 8 weeks postinjection, and these improvements were significantly greater in animals injected with PPy-chitosan (***P*<0.01 vs saline, # *P*<0.05 vs chitosan). **H**, Representative P–V loops for saline-, chitosan-, and PPy-chitosan–injected hearts. In the comparison of the mean values, chitosan injection significantly improved the end-systolic P–V relationship (**I**) and the preload recruitable stroke work (**J**) in comparison with the injection with saline, and injection with PPy-chitosan further improved these parameters significantly in comparison with ungrafted chitosan (***P*<0.01 among all 3 groups). The slopes of the end-systolic P–V relationship were significantly different between the PPy-chitosan and saline control groups, whereas the slope of the preload recruitable stroke work analysis was significantly different between the saline-injected group and both biomaterial groups (##*P*<0.01 vs saline control).

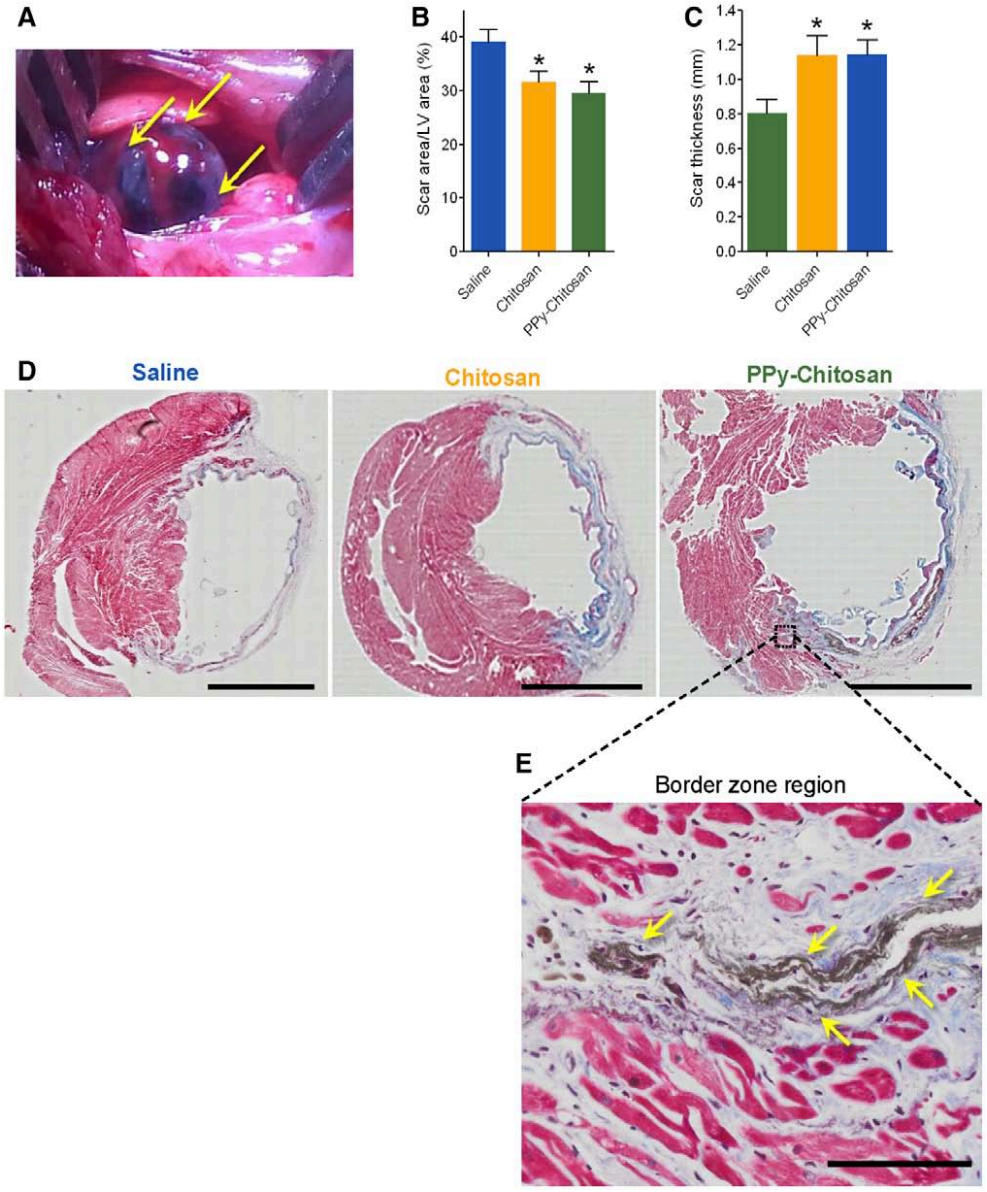

Figure 6. Hydrogel-injected hearts had smaller scars. Saline, chitosan, or PPy-chitosan was injected into the border zone of rats 1 week post-MI. **A**, Intraoperative photograph, showing 3 darker areas of PPy-chitosan injected into the border zone (arrows). Eight weeks after injection, hearts were excised and scar area and thickness were measured (saline, n=6; chitosan, n=8; PPy-chitosan, n=8). PPy-chitosan– and chitosan-treated hearts had similar scar areas (**B**) and scar thicknesses (**C**) and were significantly different than saline-treated hearts (*P<0.05). Scale bar=3 mm. **D**, Representative heart sections from each experimental group from a comparable transverse section landmarked just below the papillary muscles. **E**, Masson trichrome staining of a representative PPy-chitosan–injected heart 8 weeks postinjection. PPy-chitosan particles can be seen in the scar and border zone (arrows). Scale bar, 100 μm.

We also have not firmly established how PPy-chitosan improved function in post-MI hearts. The conductive polymer could have increased impulse propagation in the infarcted heart similar to the increase we found with neonatal cardiomyocytes, but future studies will be required to determine the mechanisms responsible for the beneficial effects we detected. The change in infarct shape identified with the conductive polymer may have resulted from the prevention of apoptotic cell death, stimulation of endogenous stem cells, or other endogenous regenerative mechanisms. Although enhanced impulse propagation is an attractive new potential target, additional research will be required to elucidate the mechanisms by which this conductive polymer improves heart function.

Conclusions

This study suggests that the conductive PPy-chitosan polymer improved cardiac function following a MI. This beneficial effect was associated with faster transverse conduction velocities in the PPy-chitosan polymer-injected rats than in either the saline control group or the group treated with chitosan alone. These in vivo results were consistent with our in vitro studies demonstrating that PPy-chitosan did not adversely affect attachment and proliferation of human cells and promoted electric conduction between tissues at a distance ex vivo. This new conductive polymer is an important advance that might someday be used clinically to improve myocardial tissue engineering to enhance regeneration postinfarction.

Acknowledgments

We thank Martin Lam for his help with the optical mapping experiments and Dr Cedric Manlhiot, Managing Director of the Cardiovascular Data Management Center at the Hospital for Sick Children and the Department of Cardiac Surgery of University of Toronto, for his assistance with the repeated measures linear regression analysis.

Sources of Funding

This work was supported by a grant from the Heart and Stroke Foundation of Ontario (G140005765). Dr Li holds a Canada Research Chair in cardiac regeneration. A. Mihic was supported by a studentship award from the Heart & Stroke/Richard Lewar Centres of Excellence in Cardiovascular Research, and an Ontario Graduate Scholarship from the province of Ontario. This work was also supported by a generous contribution by Eileen Mercier.

Disclosures

None.

References

1. Go AS, Mozaffarian D, Roger VL, Benjamin EJ, Berry JD, Blaha MJ, Dai S, Ford ES, Fox CS, Franco S, Fullerton HJ, Gillespie C, Hailpern SM, Heit JA, Howard VJ, Huffman MD, Judd SE, Kissela BM, Kittner SJ, Lackland DT, Lichtman JH, Lisabeth LD, Mackey RH, Magid DJ, Marcus GM, Marelli A, Matchar DB, McGuire DK, Mohler ER 3rd, Moy CS, Mussolino ME, Neumar RW, Nichol G, Pandey DK, Paynter NP, Reeves MJ, Sorlie PD, Stein J, Towfighi A, Turan TN, Virani SS, Wong ND, Woo D, Turner MB; American Heart Association Statistics Committee and Stroke Statistics Subcommittee. Executive summary: heart disease and stroke statistics–2014 update: a report from the American Heart Association. *Circulation*. 2014;129:399–410. doi: 10.1161/01.cir.0000442015.53336.12.
2. Ruschitzka F, Abraham WT, Singh JP, Bax JJ, Borer JS, Brugada J, Dickstein K, Ford I, Gorcsan J 3rd, Gras D, Krum H, Sogaard P, Holzmeister J; EchoCRT Study Group. Cardiac-resynchronization therapy in heart failure with a narrow QRS complex. *N Engl J Med*. 2013;369:1395–1405. doi: 10.1056/NEJMoa1306687.
3. Rane AA, Christman KL. Biomaterials for the treatment of myocardial infarction: a 5-year update. *J Am Coll Cardiol*. 2011;58:2615–2629. doi: 10.1016/j.jacc.2011.11.001.
4. Shen D, Wang X, Zhang L, Zhao X, Li J, Cheng K, Zhang J. The amelioration of cardiac dysfunction after myocardial infarction by the injection of keratin biomaterials derived from human hair. *Biomaterials*. 2011;32:9290–9299. doi: 10.1016/j.biomaterials.2011.08.057.
5. Leung BM, Miyagi Y, Li R-K, Sefton MV. Fate of modular cardiac tissue constructs in a syngeneic rat model (published online ahead of print March 15, 2013). *J Tissue Eng Regen Med*. doi: 10.1002/term.1724.
6. Blackburn NJ, Sofrenovic T, Kuraitis D, Ahmadi A, McNeill B, Deng C, Rayner KJ, Zhong Z, Ruel M, Suuronen EJ. Timing underpins the benefits associated with injectable collagen biomaterial therapy for the treatment of myocardial infarction. *Biomaterials*. 2015;39:182–192. doi: 10.1016/j.biomaterials.2014.11.004.
7. Leor J, Tuvia S, Guetta V, Manczur F, Castel D, Willenz U, Petneházy O, Landa N, Feinberg MS, Konen E, Goitein O, Tsur-Gang O, Shaul M, Klapper L, Cohen S. Intracoronary injection of in situ forming alginate hydrogel reverses left ventricular remodeling after myocardial infarction in Swine. *J Am Coll Cardiol*. 2009;54:1014–1023. doi: 10.1016/j.jacc.2009.06.010.
8. Zhang X, Wang H, Ma X, Adila A, Wang B, Liu F, Chen B, Wang C, Ma Y. Preservation of the cardiac function in infarcted rat hearts by the transplantation of adipose-derived stem cells with injectable fibrin scaffolds. *Exp Biol Med (Maywood)*. 2010;235:1505–1515. doi: 10.1258/ebm.2010.010175.
9. Miller JS. The 2000 Nobel Prize in Chemistry–a personal accolade. *Chemphyschem*. 2000;1:229–230. doi: 10.1002/1439-7641(20001215)1:4<229::AID-CPHC229>3.0.CO;2-J.
10. Shirakawa H, Louis EJ, MacDiarmid AG, Chiang CK, Heeger AJ. Synthesis of electrically conducting organic polymers: halogen derivatives of polyacetylene, (CH)x. *J Chem Soc Chem Commun*. 1977;578–580.
11. Rivers TJ, Hudson TW, Schmidt CE. Synthesis of a novel, biodegradable electrically conducting polymer for biomedical applications. *Adv Funct Mater*. 2002;12:33–37.
12. Schmidt CE, Shastri VR, Vacanti JP, Langer R. Stimulation of neurite outgrowth using an electrically conducting polymer. *Proc Natl Acad Sci U S A*. 1997;94:8948–8953.
13. Huang J, Hu X, Lu L, Ye Z, Zhang Q, Luo Z. Electrical regulation of Schwann cells using conductive polypyrrole/chitosan polymers. *J Biomed Mater Res A*. 2010;93:164–174. doi: 10.1002/jbm.a.32511.
14. Kai D, Prabhakaran MP, Jin G, Ramakrishna S. Polypyrrole-contained electrospun conductive nanofibrous membranes for cardiac tissue engineering. *J Biomed Mater Res A*. 2011;99:376–385. doi: 10.1002/jbm.a.33200.
15. Ulery BD, Nair LS, Laurencin CT. Biomedical applications of biodegradable polymers. *J Polym Sci B Polym Phys*. 2011;49:832–864. doi: 10.1002/polb.22259.
16. Roughley P, Hoemann C, DesRosiers E, Mwale F, Antoniou J, Alini M. The potential of chitosan-based gels containing intervertebral disc cells for nucleus pulposus supplementation. *Biomaterials*. 2006;27:388–396. doi: 10.1016/j.biomaterials.2005.06.037.
17. Bhattarai N, Gunn J, Zhang M. Chitosan-based hydrogels for controlled, localized drug delivery. *Adv Drug Deliv Rev*. 2010;62:83–99. doi: 10.1016/j.addr.2009.07.019.
18. Gerczuk PZ, Kloner RA. An update on cardioprotection: a review of the latest adjunctive therapies to limit myocardial infarction size in clinical trials. *J Am Coll Cardiol*. 2012;59:969–978. doi: 10.1016/j.jacc.2011.07.054.
19. Sharma V, Bell RM, Yellon DM. Targeting reperfusion injury in acute myocardial infarction: a review of reperfusion injury pharmacotherapy. *Expert Opin Pharmacother*. 2012;13:1153–1175. doi: 10.1517/14656566.2012.685163.
20. Lu WN, Lü SH, Wang HB, Li DX, Duan CM, Liu ZQ, Hao T, He WJ, Xu B, Fu Q, Song YC, Xie XH, Wang CY. Functional improvement of infarcted heart by co-injection of embryonic stem cells with temperature-responsive chitosan hydrogel. *Tissue Eng Part A*. 2009;15:1437–1447. doi: 10.1089/ten.tea.2008.0143.
21. Christman KL, Fok HH, Sievers RE, Fang Q, Lee RJ. Fibrin glue alone and skeletal myoblasts in a fibrin scaffold preserve cardiac function after myocardial infarction. *Tissue Eng*. 2004;10:403–409. doi: 10.1089/107632704323061762.
22. Huang NF, Yu J, Sievers R, Li S, Lee RJ. Injectable biopolymers enhance angiogenesis after myocardial infarction. *Tissue Eng*. 2005;11:1860–1866. doi: 10.1089/ten.2005.11.1860.
23. Wu J, Zeng F, Huang XP, Chung JC, Konecny F, Weisel RD, Li RK. Infarct stabilization and cardiac repair with a VEGF-conjugated, injectable hydrogel. *Biomaterials*. 2011;32:579–586. doi: 10.1016/j.biomaterials.2010.08.098.
24. Li Z, Guan J. Hydrogels for cardiac tissue engineering. *Polymers*. 2011;3:740–761.
25. Song K, Qiao M, Liu T, Jiang B, Macedo HM, Ma X, Cui Z. Preparation, fabrication and biocompatibility of novel injectable temperature-sensitive chitosan/glycerophosphate/collagen hydrogels. *J Mater Sci Mater Med*. 2010;21:2835–2842. doi: 10.1007/s10856-010-4131-4.
26. Lü S, Wang H, Lu W, Liu S, Lin Q, Li D, Duan C, Hao T, Zhou J, Wang Y, Gao S, Wang C. Both the transplantation of somatic cell nuclear transfer- and fertilization-derived mouse embryonic stem cells with temperature-responsive chitosan hydrogel improve myocardial performance in infarcted rat hearts. *Tissue Eng Part A*. 2010;16:1303–1315. doi: 10.1089/ten.TEA.2009.0434.
27. Rutherford SL, Trew ML, Sands GB, LeGrice IJ, Smaill BH. High-resolution 3-dimensional reconstruction of the infarct border zone: impact of structural remodeling on electrical activation. *Circ Res*. 2012;111:301–311. doi: 10.1161/CIRCRESAHA.111.260943.
28. Lee LC, Wall ST, Klepach D, Ge L, Zhang Z, Lee RJ, Hinson A, Gorman JH 3rd, Gorman RC, Guccione JM. Algisyl-LVR™ with coronary artery bypass grafting reduces left ventricular wall stress and improves function in the failing human heart. *Int J Cardiol*. 2013;168:2022–2028. doi: 10.1016/j.ijcard.2013.01.003.
29. Tse HF, Xue T, Lau CP, Siu CW, Wang K, Zhang QY, Tomaselli GF, Akar FG, Li RA. Bioartificial sinus node constructed via *in vivo* gene transfer of an engineered pacemaker HCN Channel reduces the dependence on electronic pacemaker in a sick-sinus syndrome model. *Circulation*. 2006;114:1000–1011. doi: 10.1161/CIRCULATIONAHA.106.615385.
30. Lu W, Yaoming N, Boli R, Jun C, Changhai Z, Yang Z, Zhiyuan S. mHCN4 genetically modified canine mesenchymal stem cells provide biological

pacemaking function in complete dogs with atrioventricular block. *Pacing Clin Electrophysiol*. 2013;36:1138–1149. doi: 10.1111/pace.12154.
31. Kotwal A, Schmidt CE. Electrical stimulation alters protein adsorption and nerve cell interactions with electrically conducting biomaterials. *Biomaterials*. 2001;22:1055–1064.
32. Wang X, Gu X, Yuan C, Chen S, Zhang P, Zhang T, Yao J, Chen F, Chen G. Evaluation of biocompatibility of polypyrrole in vitro and in vivo. *J Biomed Mater Res A*. 2004;68:411–422. doi: 10.1002/jbm.a.20065.
33. Hsiao CW, Bai MY, Chang Y, Chung MF, Lee TY, Wu CT, Maiti B, Liao ZX, Li RK, Sung HW. Electrical coupling of isolated cardiomyocyte clusters grown on aligned conductive nanofibrous meshes for their synchronized beating. *Biomaterials*. 2013;34:1063–1072. doi: 10.1016/j.biomaterials.2012.10.065.
34. Engler AJ, Carag-Krieger C, Johnson CP, Raab M, Tang HY, Speicher DW, Sanger JW, Sanger JM, Discher DE. Embryonic cardiomyocytes beat best on a matrix with heart-like elasticity: scar-like rigidity inhibits beating. *J Cell Sci*. 2008;121(pt 22):3794–3802. doi: 10.1242/jcs.029678.
35. Bhana B, Iyer RK, Chen WL, Zhao R, Sider KL, Likhitpanichkul M, Simmons CA, Radisic M. Influence of substrate stiffness on the phenotype of heart cells. *Biotechnol Bioeng*. 2010;105:1148–1160. doi: 10.1002/bit.22647.

SUPPLEMENTAL MATERIAL

for

A conductive polymer hydrogel supports cell electrical signaling and improves cardiac function after implantation into myocardial infarct

Anton Mihic, MSc[1,2], Zhi Cui, MSc[1,2], Jun Wu, MD[1,2], Goran Vlacic, BASc[1,2], Yasuo Miyagi, MD[1,2], Shu-Hong Li, MSc[1,2], Sun Lu, MD[1,2], Hsing-Wen Sung, PhD[3], Richard D. Weisel, MD[1,2], Ren-Ke Li, MD, PhD[1,2]

[1]Division of Cardiovascular Surgery, Toronto General Research Institute, University Health Network, Toronto, Ontario, Canada; [2]Department of Surgery, Division of Cardiac Surgery, University of Toronto, Toronto, Ontario, Canada; [3]Department of Chemical Engineering, National Tsing Hua University, Hsinchu, Taiwan

Supplemental Methods

PPy-chitosan biomaterial preparation

A chemical oxidative polymerization method was employed to conjugate PPy with chitosan to create a crosslinked gel biomaterial. A 2% chitosan stock solution was prepared by dissolving chitosan powder (Sigma-Aldrich, St. Louis, MO) in deionized distilled water containing 1% (v/v) acetic acid and mechanically stirred for 12h until a clear light yellow solution was obtained. Biomaterials with three different PPy:chitosan weight/weight ratios (0:1, 3:100 and 3:10) were generated by dissolving pyrrole solution (Sigma-Aldrich) in 2% chitosan. The mixture was mechanically stirred for 10min. $FeCl_3$ (Sigma-Aldrich) was added to the PPy-chitosan mixture drop-by-drop to slowly polymerize the pyrrole. This reaction was maintained for 48h at room temperature. At the end of reaction, the mixture was dialyzed in 0.1% PBS for 12h using dialysis tubing with a molecular weight limit of 12–14,000 Da. The pH of the biomaterial was adjusted to ~6.5 using NaOH (Sigma-Aldrich). PPy-chitosan gel was formed using 0.4% glutaraldehyde (Sigma-Aldrich) solution.

Assays of the physical and electrical properties of PPy-chitosan

Compression testing was used to determine the mechanical properties of the hydrogel. Polymerized gels were prepared as disks and uniaxially compressed using a Mach-1 testing apparatus (BioMomentum, Laval, QC), and compressed to 10% of their initial thickness. The elastic modulus was determined from the experimentally determined stress-relaxation relationship (n = 4/group).

Cyclic voltammetry was used to assess the electrochemical-dependent effects of voltage cycling on observed current amplitudes from the various hydrogels. A Verastat 3 potentiostat (Princeton Applied Research, Oak Ridge, TN) was used cycle the potential from 0V to 1V, then to –1V, and back to 0 while simultaneously recording the current. Voltage ramping was performed at a constant rate of 100mV/s for three uninterrupted cycles. Hydrogel samples were crosslinked within custom-fabricated $1cm^3$ cuvettes with copper top and bottom walls, which permitted the attachment of working and reference electrodes. All recordings were performed at room temperature and hydrogel/cuvette units were used for once only (n = 5/group).

The electrical conductivity of chitosan alone and the two concentrations of PPy-chitosan was measured using the four-probe method with two pairs of contacts as previously described[1]. The conductivity (measured in S/cm) is calculated as $1/[2\pi D(V/I)]$ where D is the distance between probes (mm), I is the supplied current (mA) and V is the corresponding voltage (mV) (n = 6/group). For all subsequent experiments, 3:10 PPy:chitosan was used, and is hereafter referred to as PPy-chitosan.

Biocompatibility of PPy-chitosan

Smooth muscle cells (SMCs) were isolated from rat aortas, and cultured in Iscove's modified Dulbecco's medium, with 10% fetal bovine serum (FBS), 100U/mL penicillin G, and 100µg/mL streptomycin (Life Technologies, Carlsbad, CA). SMCs were plated at a concentration of 250 cells/mm^2 to assess cell attachment. SMCs were grown on uncoated polystyrene dishes or those coated with chitosan or PPy-chitosan. After 48h, cells were fixed with 2% paraformaldehyde (Sigma-Aldrich) and stained with 4',6-diamidino-2-phenylindole (DAPI, Sigma-Aldrich) to visualize

cell nuclei and to facilitate counting. Images were acquired with an Eclipse Ti microscope (Nikon, Tokyo, Japan).

SMCs were then grown on uncoated glass coverslips, or hydrogel-coated coverslips. After 48h, these were fixed with 2.5% glutaraldehyde and subsequently post-fixed with OsO_4 (Sigma-Aldrich) for 30min to facilitate imaging using scanning electron microscopy (SEM) as previously dexcribed[2]. Samples were dehydrated with ethanol, dried with a critical point drier (Tousimis, Rockville, MD), and then gold sputter-coated (Polaron Instruments, Laughton, UK) before images were obtained with a Hitachi S3400N SEM (Hitachi Canada, Mississauga, ON). All images were obtained at an acceleration voltage of 15kV, a chamber pressure of 10^{-5}torr, and a direct magnification of 950×.

To measure proliferation, rat SMCs were plated on polystyrene alone, chitosan, or PPy-chitosan at a density of 50 cells/mm^2. Cells were counted as above using DAPI after 2, 5 or 10 days in culture.

To assess general SMC metabolism, an MTT kit was purchased from EMD Millipore (Billerica, MA) and used according to the manufacturer's instructions. Briefly, a total of 1×10^4 SMCs were seeded on polystyrene, chitosan or PPy-chitosan plates, and grown for 48h. SMCs were incubated with MTT for 3h at 37°C, and overall cellular metabolism was determined by measuring a test wavelength of OD 570nm and a reference wavelength of 630nm.

Ex vivo *measurement of bioconductivity between isolated skeletal muscle*

All animal protocols were approved by the Animal Care Committee of the University Health Network. Rat leg skeletal muscle (*biceps femoris*) segments were isolated from the hindlimbs of adult Sprague-Dawley rats (Charles River Canada, St-Constant, QC) and trimmed to ensure that both specimens were of the same weight (1.0–1.2g). Two segments were plated 25mm apart on 60mm dishes coated with chitosan or PPy-chitosan. A 3-lead electromyogram (EMG) recorder (Power Lab, ADInstruments, Colorado Springs CO) was used to obtain action potentials from one set of muscles, while two stimulating electrodes connected to an electrical stimulator (Grass Technologies, Warwick, RI) were connected to the opposing muscle. Stimulation involved pacing the muscles at a constant voltage for 10s at 1Hz with 14ms duration and gradually ramping the voltage amplitude every 10s from 0.1V to 10V. Notations were made in the recording software to denote each step in voltage. The peak amplitude (measured in mV) from the corresponding muscle was obtained using Lab Chart software (AdInstruments) for n = 6 experiments/group.

In addition to the two-muscle recording procedures, one muscle segment was excited using non-contact stimulation. This consisted of placing a positive electrode directly in the muscle, with the positive electrode placed into the hydrogel at a distance of 8mm. Stimulation was gradually ramped from 0.1V until a contractile response was elicited and could be visually detected in the muscle.

Isolation of neonatal rat cardiomyocytes

Neonatal rat cardiomyocytes were isolated from 1-day-old Sprague-Dawley rats of either sex using enzymatic dissociation. Fourteen hearts were collected from neonates and minced in ice-cold PBS supplemented with 10g/L glucose. Minced heart tissue was digested with 4mL of enzymes mixture composed of trypsin, DNAnase, and collagenase. The mixture was gently agitated at 37°C for 8min.

At the end of each digestion cycle, the supernatant (containing cells) was transferred into a sterile bottle with 20mL Dulbecco's modified Eagle's medium/Ham's F-12 (DF-12) medium supplemented with 20% FBS (Life Technologies). Ten digestion cycles were performed. Cells were collected and purified using Percoll (GE Healthcare Canada, Mississauga, ON). Purified cardiomyocytes were cultured in DF-12 medium supplemented with 10% FBS with an initial seeding density of 3×10^5.

Ca^{2+} transient and voltage-sensitive dye imaging system

Ca^{2+} transient of cardiomyocytes and electrical conduction of Langendorff-perfused rat hearts containing voltage-sensitive dyes were measured using a commercially available optical high-speed electron-multiplied charge-coupled device (EMCCD) camera system (Evolve 128, Photometrics, Tucson, AZ). The camera was coupled to a dissecting microscope mounted vertically on a boom for Ca^{2+} transient measurement and horizontally for Langendorff-perfused rat heart imaging. Cardiomyocytes were loaded with the cell-permeable Ca^{2+} indicator Fluo-4 AM (5μM, Life Technologies) for 30min and washed with Tyrode's solution. Fluo-4 AM was excited at 488nm and emission at > 515nm was detected. For voltage-imaging with Langendorff-perfused rat hearts, di-4-ANEPPS (Life Technologies) was excited at 494nm and emission at 516nm was detected. Fluorescent excitation and emission of di-4-ANNEPS was achieved with a D530/20 exciter, a 565dcxr beam splitter and a D605/55 emitter (Chroma Technology, Bellows Falls, VT). The fluorescent images of Ca^{2+} transient were recorded using a high-speed EMCCD camera at 485 frames/s (128×128 pixels) with a resolution of 60.5μm/pixel, while the voltage-sensitive dye images of Langendorff-perfused rat hearts were recorded at 883 frames/s (64×64 pixels) with a resolution of 96.5μm/pixel. Images were obtained using Micromanager and ImageJ (NIH, Bethesda, MD) and data analysis was performed using ImageJ and BV_Analyze software (BrainVision, Morrisville, NC). Sequences of interest containing visible fluorescence were processed by applying a Butterworth low-pass filter at 100Hz, and by subsequently detecting the peak of activation. The

first derivative of the maximal activation (dF/dT_{max}) was used to create isochronal maps for both neonatal cardiomyocyte monolayers and rat hearts. For video sequences, a rolling average subtraction and median filtering followed by pseudo-coloring was used to visually identify the propagation of electrical signals in the rat hearts. These pseudo-colored sequences were superimposed onto the raw video sequences to aid in the determination of cardiac anatomy with respect to electrical activity.

Acute MI model and experimental timeline

The permanent MI model used in this study has been extensively tested in our lab[3,4]. Female Sprague-Dawley rats (weighing 225–250g) were anesthetized, intubated and ventilated with 2% isoflurane (Pharmaceutical Partners of Canada, Richmond Hill, ON) mixed with oxygen. The chest was opened by a lateral thoracotomy, and a single 7-0 prolene suture stitch was introduced around the left descending coronary artery and tightened. The infarct area was observed as a pale region on the front of the heart. The chest was then closed and the animal allowed to recover for 1 week. This acute infarct model has previously been shown to create infarcts that comprise ~35% of the left ventricle (LV).

Biomaterial injection

One week after MI, rats with a fractional shortening of 25–35% by echocardiography (ECHO) were pre-selected and then randomized into chitosan-, PPy-chitosan- (n = 8/group), or control saline-injected (n = 6) groups. The animals were anesthetized, intubated, ventilated and the chest was opened by a lateral thoracotomy. A total volume of 100μL was injected into 3 peri-infarct LV regions of each heart (33μL/region) using a 500μL tuberculin syringe and a 28-gauge needle (BD Biosciences, Mississauga, ON). The chest was then closed and the animal allowed to recover. Eight weeks after injection, the rats were euthanized with an isoflurane overdose (5%).

Evaluation of electrocardiogaphy (ECG) and cardiac function

ECG was measured prior to infarction (–1), at the time of biomaterial injection (0), and 1, 2, 3, 4, 6 and 8 weeks after injection. Briefly, rats were anesthetized with 2–3% isoflurane and allowed to equilibrate for 10min. Five minute recordings were obtained using three surface leads (positive, negative, reference) and recorded using the Power Lab software (AdInstruments). Recordings were analyzed using Lab Chart (AdInstruments) and the 5min sequences were averaged to obtain standard ECG wave intervals and durations.

Cardiac function was evaluated using two techniques: echocardiography (ECHO) at several time points after MI, and pressure–volume (P–V) analysis at the end point, as previously described[3,4]. In brief, LV function was evaluated by ECHO prior to infarction (–1), at the time of biomaterial injection (0), and 2, 4 and 8 weeks after injection. M- and B-mode images were obtained in the parasternal short axis at the level of the papillary muscle tips. For each measurement, 3 consecutive cardiac cycles were recorded and averaged by a single examiner blind to the animal's experimental group. Left ventricular internal systolic dimension (LVIDS) and left ventricular internal diastolic dimension (LVIDD) were determined in M-mode imaging. In B-mode imaging, the left ventricular end diastolic area (LVEDA) was determined as the largest cavity size, and left ventricular end systolic area (LVESA) as the smallest. Percent fractional shortening (%FS) and percent fractional area change (%FAC) were calculated as follows: %FAC = [(LVEDA-LVESA)/LVEDA) × 100] and% FS = [(LVIDD-LVISD)/LVIDD) × 100]. Percent ejection fraction (% EF) was calculated as follows: $[(LVIDD^3\text{-}LVISD^3)/LVIDD^3) \times 100$.

Eight weeks after biomaterial injection, cardiac function was further evaluated using a P–V catheter system. Briefly, under general anesthesia, a 2.0F micromanometer and conductance catheter (SPR-

838, Millar Instruments, Houston, TX), which can simultaneously measure LV pressure and volume in rats, was introduced into the LV through the right carotid artery. Cardiac function (% EF, dP/dt, preload recruitable stroke work and end-systolic P–V relationship) and LV volumes were computed using the PVAN software (Millar Instruments). Once functional evaluations were completed, hearts from each group were fixed in 10% formalin at physiologic pressure for morphometric and histological analyses.

Langendorff-perfusion of isolated rat hearts

Hearts (n = 8 for chitosan- and PPy-chitosan-treated groups and n = 6 for the saline control) were retrieved after the animals were heparinized and euthanized by isoflurane overdose. To cease the heartbeat and preserve cells during ischemia, hearts were retrograde-perfused with ice-cold cardioplegia solution (140mM NaCl, 4mM Tris, 30mM KCl, 5mM $MgSO_4$, 25mM dextrose and 30mM histidine, pH 7.15) and cannulated using a blunted 27G needle *via* the aortic root. Hearts were then perfused on ice with the voltage-sensitive dye di-4-ANEPPS dissolved in cardioplegia solution (25μM) at a rate of 5mL/min for 6min. Hearts were mounted on a customized Langendorff apparatus and perfused with Krebs Henseleit solution (117mM NaCl, 24mM $NaHCO_3$, 11.5mM dextrose, 3.3mM KCl, 1.25mM $CaCl_2$, 1.2mM $MgSO_4$, 1.2mM KH_2PO_4 and buffered with 5% CO_2/95% O_2 gas) at 37^0C at a rate of 5mL/min. To prevent motion noise, excitation-contraction coupling was blocked using blebbistatin (5μM, Sigma-Aldrich).

Following optical mapping experiments, rat hearts were fixed in diastole with 1M KCl and fixed in 10% formalin for 5 days. Hearts were then embedded in paraffin, cross-sectioned and stained with Masson's trichrome. Whole heart cross-sections were scanned with a 20× objective using a VS120 slide scanner (Olympus). Cardiac cross sections were analyzed in the same transverse plane below

the papillary muscles, and the CellSens software (Olympus Canada, Richmond Hill, ON) was used to measure scar thickness: LV area and scar area: LV area ratios.

Statistical Analysis

Data are expressed as mean ± SEM. Student's *t*-tests were used for comparisons of means between two groups. Comparisons of means among three or more groups were done by ANOVA. If the F ratio was significant, post-hoc tests were performed to specify which groups were significantly different. A one-way Tukey post-hoc test was employed when the experimental groups had the same *n* values, namely the *in vitro* MTT and cell calcium transit velocity analyses. When *n* values were not equal between experimental groups, the Bonferroni post-hoc test was used. One-way Bonferroni tests were used for ejection fraction, dPdt Max, dPdt Min, heart scar area and heart scar thickness analyses. Since a Levene's test for equality of variances showed some variances were not equal, a one-way Welch's ANOVA followed by Tamhane's T2 post-hoc testing was used for the biomaterial conductivity assay and an unpaired *t*-test with Welch's correction was used for the analysis of action potential amplitude in the skeletal muscle stimulation assay. For the ECG and echocardiography analysis, which consisted of repeated measures of the same animals over time, linear regression models adjusted for repeated measures through a compound symmetry covariance structure were used to generate general estimating equations with the maximum likelihood estimate method for parameter estimation. As appropriate, baseline values (prior to intervention) were added as obligatory covariates in all regression models. Two sets of regression models were created, one directly comparing average values among the 3 groups and one also comparing the slope of change over time. An additional set of regression models was created with Dunnett-Hsu adjustment for multiple comparison but results were not reported since the statistical significance remained similar between adjusted and unadjusted models. The load-independent

measurements of ventricular function were analyzed by linear regression models adjusted for repeated measures in the same fashion, and both means and slopes were compared. Differences were considered statistically significant at $p < 0.05$. Statistical analyses were done using SAS v9.3 (SAS Institute, Cary NC) for the linear regression models, SPSS 23 (IBM, Armonk, NY) for the Welch's ANOVA and GraphPad Prism 5 (GraphPad, La Jolla, CA) for all other analyses.

References

1. Marcasuzaa P, Reynaud S, Ehrenfeld F, Khoukh A, Desbrieres J. Chitosan-graft-polyaniline-based hydrogels: elaboration and properties. *Biomacromolecules*. 2010;11:1684–1691.

2. Mihic A, Li J, Miyagi Y, Gagliardi M, Li S-H, Zu J, Weisel RD, Keller G, Li R-K. The effect of cyclic stretch on maturation and 3D tissue formation of human embryonic stem cell-derived cardiomyocytes. *Biomaterials*. 2014;35:2798–2808.

3. Tian H, Huang M-L, Liu K-Y, Jia Z-B, Sun L, Jiang S-L, Liu W, McDonald Kinkaid HY, Wu J, Li R-K. Inhibiting matrix metalloproteinase by cell-based timp-3 gene transfer effectively treats acute and chronic ischemic cardiomyopathy. *Cell Transplant*. 2012;21:1039–1053.

4. Wu J, Zeng F, Huang X-P, Chung JC-Y, Konecny F, Weisel RD, Li R-K. Infarct stabilization and cardiac repair with a VEGF-conjugated, injectable hydrogel. *Biomaterials*. 2011;32:579–586.

Supplementary Video Legends

Supplementary Video 1: Optical mapping of electrical conduction in a healthy rat heart. Raw video (left) and pseudocolored electrical propagation (middle) of a Langendorff-perfused heart from a health animal (without myocardial infarction) are superimposed (right).

Supplementary Video 2: Optical mapping of electrical conduction in a rat heart injected with saline 1 week post-MI. Raw video (left) and pseudocolored electrical propagation (middle) of a Langendorff-perfused heart from a saline-injected animal are superimposed (right).

Supplementary Video 3: Optical mapping of electrical conduction in a rat heart injected with chitosan 1 week post-MI. Raw video (left) and pseudocolored electrical propagation (middle) of a Langendorff-perfused heart from a chitosan-injected animal are superimposed (right).

Supplementary Video 4: Optical mapping of electrical conduction in a rat heart injected with PPy-chitosan 1 week post-MI. Raw video (left) and pseudocolored electrical propagation (middle) of a Langendorff-perfused heart from a PPy-chitosan-injected animal are superimposed (right).

A Conductive Polymer Hydrogel Supports Cell Electrical Signaling and Improves Cardiac Function After Implantation into Myocardial Infarct

Anton Mihic, Zhi Cui, Jun Wu, Goran Vlacic, Yasuo Miyagi, Shu-Hong Li, Sun Lu, Hsing-Wen Sung, Richard D. Weisel and Ren-Ke Li

Circulation. 2015;132:772-784
doi: 10.1161/CIRCULATIONAHA.114.014937
Circulation is published by the American Heart Association, 7272 Greenville Avenue, Dallas, TX 75231

Print ISSN: 0009-7322. Online ISSN: 1524-4539